Applied Physics Letters

RESEARCH ARTICLE | MAY 16 2022

Photocurrent detection of radially polarized optical vortex with hot electrons in Au/GaN

Yaonan Hou ; Menno Kappers; Chaoyuan Jin; Rachel Oliver

Appl. Phys. Lett. 120, 202101 (2022)
https://doi.org/10.1063/5.0094454

Applied Physics Letters ARTICLE scitation.org/journal/apl

Photocurrent detection of radially polarized optical vortex with hot electrons in Au/GaN

Cite as: Appl. Phys. Lett. **120**, 202101 (2022); doi: 10.1063/5.0094454
Submitted: 3 April 2022 · Accepted: 4 May 2022 ·
Published Online: 16 May 2022

Yaonan Hou,[1,a)] Menno Kappers,[2] Chaoyuan Jin,[3,4] and Rachel Oliver[2]

AFFILIATIONS

[1]Optoelectronics Research Centre, The University of Southampton, Southampton SO17 1BJ, United Kingdom
[2]Department of Materials Science and Metallurgy, University of Cambridge, 27 Charles Babbage Road, Cambridge CB3 0FS, United Kingdom
[3]College of Information Science and Electronic Engineering, Zhejiang University, Hangzhou 310027, China
[4]Department of Electronic and Electrical Engineering, University of Sheffield, Sheffield S3 7HQ, United Kingdom

[a)]Author to whom correspondence should be addressed: yaonan.hou@soton.ac.uk

ABSTRACT

We report a GaN based metal–semiconductor–metal (MSM) infrared photodetector enabled with azimuthally distributed sub-wavelength gratings fabricated on one of the working electrodes. Under illumination, hot electron transfer is introduced by the plasmonic resonance in the infrared waveband formed at the interface of Au/GaN. Without the help of using any external optical polarizers, the device is able to detect radial polarization vortices in the form of photocurrents with a prescribed response spectrum. The detector exhibits a 10%–90% rise and fall time of 0.9 ms under modulated light, much faster than that of conventional ultraviolet GaN MSM photodetectors based on the band edge absorption. This work provides a viable way to measure spatially variant polarization beams with a compact plasmonic photodetectors fabricated from wide bandgap semiconductors.

A polarization vortex associated with polarization singularities comprises of spatially varying field vectors, which plays a pivotal role in modern optics. Endowed with polarization vortices, many optical beams and pulses with unique properties have been proposed and realized, such as vector beams,[1–3] structured light coupled with orbital angular momentum,[4–6] and "doughnut" pulses,[7–9] to name a few. Amid the growing interest in new light beams and pulses, polarization vortices have found their applications in tight focusing,[10] laser machining,[11] data storage,[12] imaging,[13] advanced spectroscopy,[14] particle trapping,[15] and so on. Despite the significance of polarization vortices, the approaches to detecting them have lagged behind, especially compared with the fast developing methods for phase vortex (orbital angular momentum) detection.[16–18] Traditional characterization of polarization vortices relies on analyzing the beam's polarization by imaging its profile, e.g., by employing a linear polarizer and a camera. Obviously, such a detection system is cumbersome to handle. It would be both time- and space-saving if a polarization vortex could be directly detected by a single photodetector in the form of a photocurrent, similar to detection of a phase vortex.[18] Such a device is not only important for practical applications but also an excellent platform to investigate light–matter interactions.[19]

As is well known, a semiconductor photodetector is generally insensitive to spatially distributed polarization. Fortunately, recent advances in plasmonic hot-electron photodetectors[20] (termed as PHEPDs in the following text) shed light on designing polarization-sensitive photodetectors to measure polarization vortices. A PHEPD is composed of plasmonic nanostructures integrated with a semiconductor photodetector. The plasmonic nanostructures resonant with the incident light to generate hot electrons, which are collected at an appropriate metal/semiconductor contact to generate a photocurrent in a closed circuit. By engineering the dimensions and distributions of the plasmonic nanostructures, they can be tailored to respond to different wavelengths (spectral selectivity) and to different polarizations (polarization sensitivity).[20,21]

In this work, we develop a near-infrared (NIR) PHEPD fabricated from an n-type GaN based metal–semiconductor–metal (MSM) photodetector with Au Schottky electrodes, where the plasmonic nanostructures are integrated for hot electron generation and transfer. GaN is selected for our device because its wide bandgap (3.4 eV) can

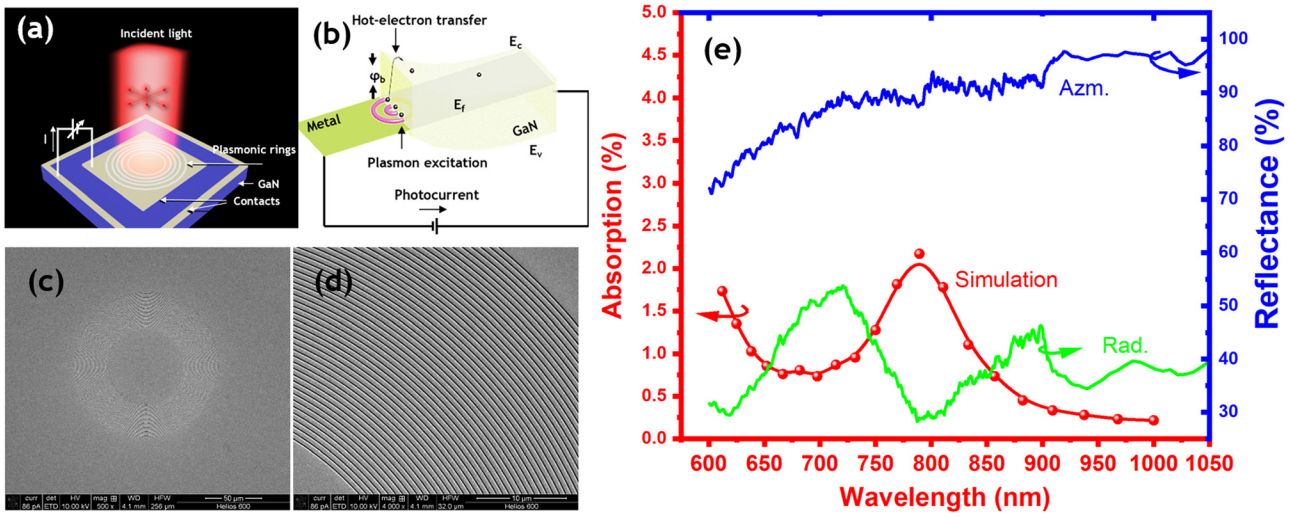

FIG. 1. (a) Schematic of the PHEPD working under radial polarized beam, where the concentric rings are the plasmonic structure fabricated on the working electrode; (b) schematic of the working mechanism of the hot electron transfer at the Au/GaN interface; (c) SEM top-view of the fabricated device; (d) zoom-in SEM images of the plasmonic structures with a good uniformity; (e) simulated spectral absorption under radial polarized light illumination (red) and experimental reflectance under radial (green) and azimuthal (blue) polarized light illumination.

act as a native filter to rule out photoelectrons generated from near bandgap absorption, leading to a net hot-electron signal. Moreover, a stable Schottky barrier can form at the Au/GaN interface as a good electron collector, benefiting from the good chemical stability and reliable doping of GaN. Therefore, the metal/GaN system is often regarded as an excellent platform to study the behaviors of hot carriers.[22–24] Moreover, the MSM architecture is suitable for photonic integrated circuits because of the feasibility in planar integration technologies. Regarding the plasmonic nanostructures, periodic rings are utilized to form concentric gratings. The entire device structure is schematically displayed in Fig. 1(a). Accordingly, the working principle is shown in Fig. 1(b), where the hot electrons are generated by the concentric ring gratings under illumination and collected by the Au/GaN Schottky barrier as photocurrent in a closed circuit.

The 1.1 μm-thick n-type doped GaN layer used in this work was grown on a (0001) sapphire substrate by metalorganic vapor-phase epitaxy (MOVPE). Hall-effect measurements showed a carrier concentration of 3.3×10^{18} /cm^3 and an electron mobility of 234 cm^2/V s. After growth, 200 nm thick Au electrodes are deposited by thermal evaporation at a rate of 0.1 nm/s under a low pressure of 1×10^{-6} mbar, following standard photolithography and liftoff processes. The MSM electrodes are defined as a concentric squares [schematically shown in Fig. 1(a) and inset of Fig. 2]. The PHEPD is finally formed by fabricating the concentric rings on the center electrode with focused ion beam (FIB) milling. Figures 1(c) and 1(d) are top-view images of scanning electron microscope (SEM) of the whole device and zoomed-in structures. The gap and period of the concentric rings are 50 and 575 nm, respectively.

The red curve with filled circles in Fig. 1(e) shows the absorbance obtained from simulation (COMSOL Multiphysics). The peak position is designed at ~790 nm, corresponding to the emission wavelength of the laser used in this experiment. The spectral reflectance of our PHEPD was first performed to examine the optical property. As shown in Fig. 1(e), in contrast to the radial polarized light being reflected, the azimuthal polarized light exhibits a prominent dip at the same position with a Q-factor of 7.2, similar to the simulated absorbance curve (Q = 9.2), indicating the formation of plasmonic resonances.

Electrical properties of the PHEPD are measured by a semiconductor parameter analyzer (Keysight B1500A) with current resolution down to 0.1 fA. Figure 2 displays the current–voltage (IV) characteristics of our device. The IV curve verifies that the device is a typical MSM PD comprising a pair of back-to-back Schottky contacts, with a dark current of 69 mA under 3 V. In order to have a deeper insight of the carrier transport, a single Schottky contact was fabricated by depositing an indium Ohmic contact in addition to Au. The whole

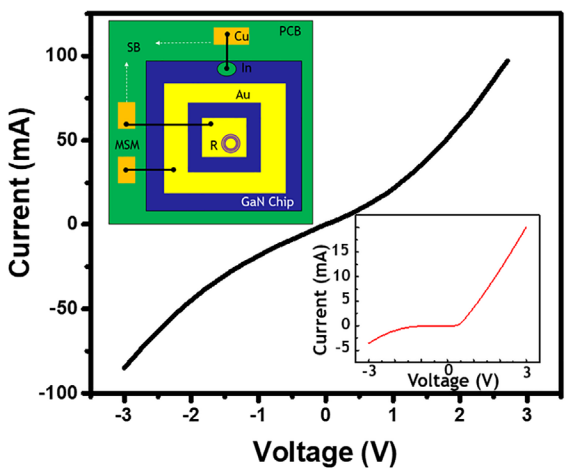

FIG. 2. IV curve of the PHEPD. Top-left inset: lay-out of the chip, where "SB" indicates the single Schottky contact formed between Au/GaN and In/GaN. Bottom-right: IV curve of the single Schottky diode.

chip is wire-bonded to a printed circuit board (PCB), as shown in the layout in the top-left inset of Fig. 2. A typical IV curve of the single Schottky contact is shown in the bottom-right inset of Fig. 2, with a turn-on voltage at ~0.5 V. The electron transport of a Schottky barrier can be described by

$$I = I_0\left[\exp\frac{eV}{nkT} - 1\right], \tag{1}$$

where n, k, and T are ideality factor, Boltzmann constant, and absolute temperature, respectively. I_0 is the reverse saturation current,

$$I_0 = AA^*T^2\exp\left(\frac{e\phi_b}{kT}\right), \tag{2}$$

where A is the contact area, A^* is the Richardson constant (26 A cm^{-2} K^{-2} for GaN), and ϕ_b is the barrier height. From Eq. (2), the barrier height ϕ_b is calculated as 0.61 eV, which is less than that of incident photon energy (1.55 eV), allowing the photo-excited hot electrons with enough energy to be emitted into the semiconductor side to form measurable photocurrents. The ideality factor of $n = 1.58$ is obtained from Eq. (1). When $n > 1$, other carrier transport mechanisms may co-exist with thermionic emission. In our case, it is attributed to the tunneling of electrons permitted by the relatively thin space-charge region (~10 nm) given by $w = \sqrt{\frac{2\phi_b}{eN_D}}$ (N_D is the doping concentration).

The optoelectronic properties of our PHEPD are characterized with a testing system schematically shown in Fig. 3(a). The system is equipped with a continuous-wave (cw) laser with an emission spectrum centered at 790 nm. A $\lambda/2$ wave plate (WP) along with a polarization converter (Edmund Optics) is used to control the polarization states. Then, the excitation beam is sent to an 20× objective lens to be focused on the sample. Before the objective lens, a beam splitter (BS) is used to monitor the incident power (with a power meter) and to align the sample (with a polarization camera). The generated photocurrent is recorded by a Keithley 2636 source meter. The polarization camera can be used to confirm the polarization states by reflecting the illumination light to the camera from the beam splitter. The image under "intensity mode" (where the camera only detects the light intensity) is shown in the center of Fig. 3(b), where the beam exhibits a donut shape. By changing the relative angle between wave plate and polarization converter, radial polarization [left column of Fig. 3(b)] and azimuthal polarization [right column of Fig. 3(b)] can be obtained under "quad-view mode" (where the polarization states will be detected by the camera), where the arrows indicate the polarization orientations of the pixels. The photocurrent, defined as the difference between total current and dark current (i.e., $I_{ph} = I_{tot} - I_{dark}$), along with the photoresponsivity as a function of applied bias under different polarizations is shown in Fig. 3(c). Obviously, the photocurrent/photoresponsivity is undetectable under azimuthal or linear polarized light illumination.

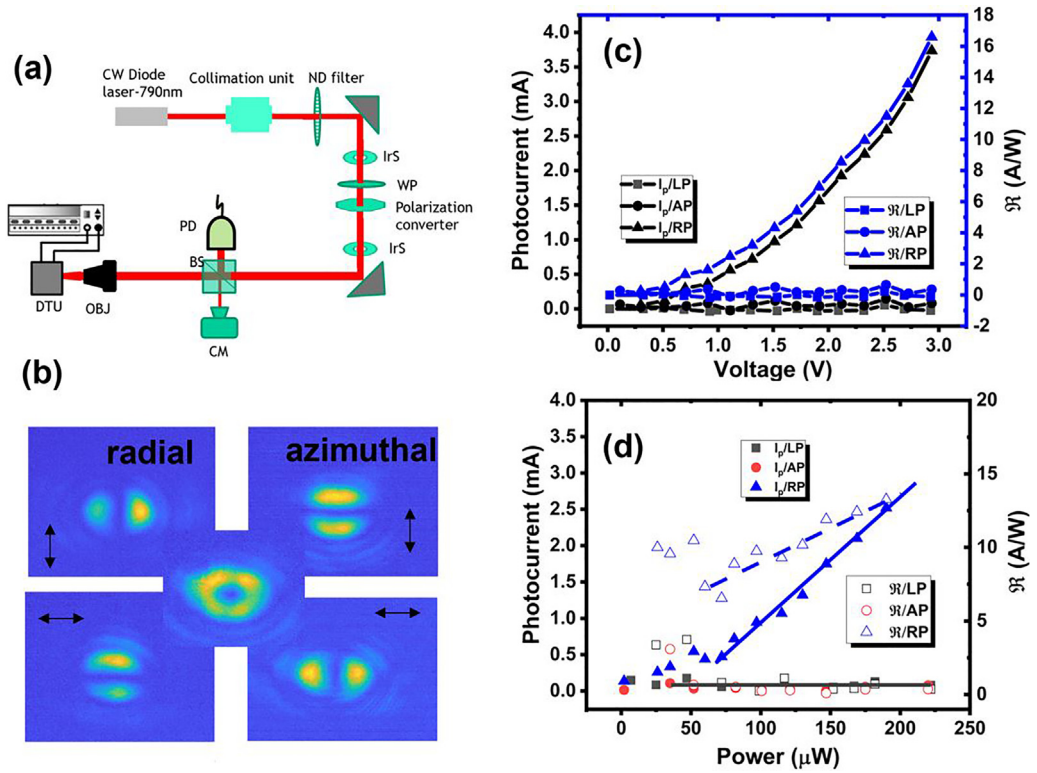

FIG. 3. (a) Schematic of the characterization system, where WP is wave plate, BS is the beam splitter, PD is the power meter, and CM is the alignment camera. (b) Confirmed donut-shape beam after the polarization converter with radial or azimuthal polarizations. (c) Photocurrent/photoresponsivity ($\mathscr{R}$) as a function of voltage under various polarized light illuminations. (d) Power-dependent photocurrent/photoresponsivity measurements under various polarized light illuminations (colored lines are guides to eyes, LP: linear polarization, AP: azimuthal polarization, RP: radial polarization).

In contrast, the photocurrent/photoresponsivity shows a nonlinear relationship with the increasing bias. Under the incident power of 225 μW, the photoresponsivity is calculated to be as high as 16.7($\pm$5%) A/W at 3 V. The large photoresponse (often associated with a high quantum efficiency and large internal gain) in GaN MSM photodetectors has previously been observed and has been attributed to various reasons, e.g., ultra-small gap between electrodes,[25] surface states,[26] and reduced-Schottky barrier under illumination.[27,28] In our case, it is likely due to the latter reasons because of the nonlinear relationship between photocurrent and applied bias. This point would be worthy of more detailed investigation in the future. At least, this work indicates that a large photocurrent response is achievable with plasmonic hot electrons. We also noticed that the photocurrent contrast ratio (photocurrent under radial polarization over that of dark current) is low (~0.05) because of the high dark current, which leads to a sub-mA variation under unwanted polarization [linear and azimuthal polarization in Fig. 3(c)]. Therefore, we undertook further investigation of the power dependent photoresponse. As shown in Fig. 3(d), the photocurrent/photoresponsivity under linear or azimuthal polarized light illumination is much lower compared with that under radial polarized light illumination, as expected. When the incident power is above 75 μW under radially polarized light illumination, the photocurrent/photoresponsivity is proportional to the incident power. Below 75 μW, it is hard to determine the value of photocurrent due to the large dark current [Fig. 3(d)].

In addition to the cw illumination, the performance of our PHEPD is investigated under ultrafast pulses using an Ti:sapphire laser (with the peak wavelength of 800 nm, a linewidth of 104 nm, and a repetition rate of 80 Hz) as the excitation source. Under 225 μW illumination, the device exhibits a 2.5 mA photocurrent under radial polarization; and no photocurrent is observed under linear Gaussian or azimuthally polarized pulses.

The transient response of the PHEPD is studied with an optical chopper and an oscilloscope. As shown in Fig. 4, the modulation speed changes from 6.6 to 132 Hz, and no signal degradation can be observed with the fastest modulation speed obtainable in our current setup. The 10%–90% rise and fall times decrease with the increasing modulation frequency (e.g., 18 ms at 6.6 Hz and 0.9 ms at 132 Hz), indicating that the limitation is the speed of beam chopping method. Therefore, it is concluded that the photocurrent decay time is faster than 0.9 ms. This is unlike the conventional GaN MSM photodetectors based on band edge absorption, which exhibit a slow photocurrent decay time up to hundreds of seconds.[29] While the mechanism of slow photocurrent decay (also referred to persistent photocurrent) is still under debate in various wide bandgap semiconductor based photodetectors,[30–32] our work suggests that a design based on a hot-electron photodetector is an option to avoid it.

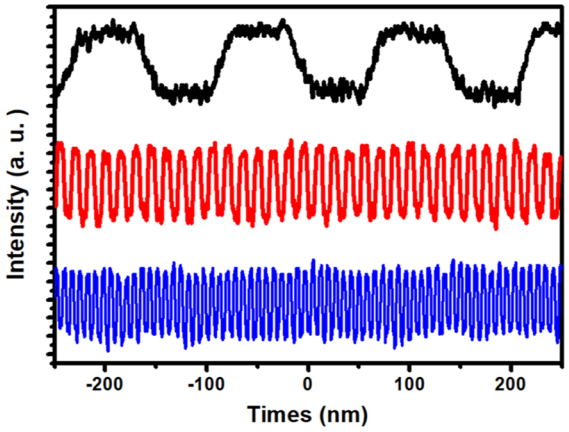

FIG. 4. Transient response of the PHEPD at the modulation speed from 6.6 (black curve) to 132 Hz (blue curve). The curves are shifted for a better comparison. Small overshot of the signal can be attributed to the system stability.

In summary, we demonstrated a hot-electron photodetector based on GaN enabled by metallic metasurfaces fabricated on a MSM structure, which is sensitive to the radially polarized vortex only. The photoresponsivity is as high as 16.7($\pm$5%) A/W under radial polarization, while near zero photoreponse can be observed under linear or azimuthal polarizations. In addition, the device exhibits a fast transient photoresponse (with a speed faster than 0.9 ms) compared with conventional GaN MSM photodetectors based on band edge absorption. We believe that our work provides useful information for fabricating high-performance spatially polarization-sensitive photodetectors with a fast response, which will be useful to study vortex currents and polarization singularities.

Y.H. and C.J. are grateful for the support by Research Stimulus Fund at the Zepler Institute for Photonics and Nanoelectronics, the University of Southampton. This work was partly supported by QUantum Dot On Silicon systems for communications, information processing and sensing (QUDOS) under the Grant No. EP/T028475/1 from Engineering and Physical Sciences Research Council (EPSRC), UK. Y.H., M.K., and R.O. appreciate the Pump-priming Program from EPSRC National Epitaxy Facility, UK. Y.H. specially thanks Dr. Nikitas Papasimkis and Professor Nikolay I. Zheludev from University of Southampton for helpful discussions.

AUTHOR DECLARATIONS

Conflict of Interest

The authors have no conflicts to disclose.

DATA AVAILABILITY

The data that support the findings of this study are available from the corresponding author upon reasonable request.

REFERENCES

[1]Q. Zhan, Adv. Opt. Photonics **1**, 1–57 (2009).
[2]R. Drevinskas, J. Zhang, M. Beresna, M. Gecevičius, A. G. Kazanskii, Y. P. Svirko, and P. G. Kazansky, Appl. Phys. Lett. **108**, 221107 (2016).
[3]M. Verma, S. K. Pal, S. Joshi, P. Senthilkumaran, J. Joseph, and H. Kandpal, J. Mod. Opt. **62**, 1068 (2015).
[4]H. Li, V. Rodriguez-Fajardo, P. Chen, and A. Forbes, arXiv:2005.02739 (2020).
[5]X.-L. Wang, J. Chen, Y. Li, J. Ding, C.-S. Guo, H.-T. Wang *et al.*, Phys. Rev. Lett. **105**, 253602 (2010).
[6]P. Gregg, M. Mirhosseini, A. Rubano, L. Marrucci, E. Karimi, R. Boyd, and S. Ramachandran, Opt. Lett. **40**, 1729 (2015).
[7]N. Papasimakis, T. Raybould, V. A. Fedotov, D. P. Tsai, I. Youngs, and N. I. Zheludev, Phys. Rev. B **97**, 201409 (2018).
[8]T. Raybould, V. A. Fedotov, N. Papasimakis, I. Youngs, and N. I. Zheludev, Appl. Phys. Lett. **111**, 081104 (2017).

[9]N. Papasimakis, V. Fedotov, V. Savinov, T. Raybould, and N. Zheludev, Nat. Mater. **15**, 263 (2016).
[10]G. M. Lerman and U. Levy, Opt. Express **16**, 4567 (2008).
[11]M. Kraus, M. A. Ahmed, A. Michalowski, A. Voss, R. Weber, and T. Graf, Opt. Express **18**, 22305 (2010).
[12]W.-C. Kim, N.-C. Park, Y.-J. Yoon, H. Choi, and Y.-P. Park, Opt. Rev. **14**, 236 (2007).
[13]H. Ishitobi, I. Nakamura, N. Hayazawa, Z. Sekkat, and S. Kawata, J. Phys. Chem. B **114**, 2565 (2010).
[14]N. Hayazawa, Y. Saito, and S. Kawata, Appl. Phys. Lett. **85**, 6239 (2004).
[15]Q. Zhan, Opt. Express **12**, 3377 (2004).
[16]P. Genevet, J. Lin, M. A. Kats, and F. Capasso, Nat. Commun. **3**, 1278 (2012).
[17]R. M. Kerber, J. M. Fitzgerald, D. E. Reiter, S. S. Oh, and O. Hess, ACS Photonics **4**, 891 (2017).
[18]M. L. Chen, L. J. Jiang, and W. E. Sha, Appl. Sci. **8**, 362 (2018).
[19]S. Sederberg, F. Kong, F. Hufnagel, C. Zhang, E. Karimi, and P. B. Corkum, Nat. Photonics **14**, 680 (2020).
[20]A. Sobhani, M. W. Knight, Y. Wang, B. Zheng, N. S. King, L. V. Brown, Z. Fang, P. Nordlander, and N. J. Halas, Nat. Commun. **4**, 1643 (2013).
[21]M. W. Knight, Y. Wang, A. S. Urban, A. Sobhani, B. Y. Zheng, P. Nordlander, and N. J. Halas, Nano Lett. **13**, 1687 (2013).
[22]G. Tagliabue, J. S. DuChene, A. Habib, R. Sundararaman, and H. A. Atwater, ACS Nano **14**, 5788 (2020).
[23]G. Tagliabue, J. S. DuChene, M. Abdellah, A. Habib, D. J. Gosztola, Y. Hattori, W.-H. Cheng, K. Zheng, S. E. Canton, R. Sundararaman *et al.*, Nat. Mater. **19**, 1312 (2020).
[24]G. Tagliabue, A. S. Jermyn, R. Sundararaman, A. J. Welch, J. S. DuChene, R. Pala, A. R. Davoyan, P. Narang, and H. A. Atwater, Nat. Commun. **9**, 3394 (2018).
[25]P. F. Satterthwaite, A. S. Yalamarthy, N. A. Scandrette, A. Newaz, and D. G. Senesky, ACS Photonics **5**, 4277 (2018).
[26]M. Garg, B. R. Tak, V. R. Rao, and R. Singh, ACS Appl. Mater. Interfaces **11**, 12017 (2019).
[27]S. Kunwar, S. Pandit, J.-H. Jeong, and J. Lee, Nano-Micro Lett. **12**, 91 (2020).
[28]X. Zhang, Q. Liu, B. Liu, W. Yang, J. Li, P. Niu, and X. Jiang, J. Mater. Chem. C **5**, 4319 (2017).
[29]B. Poti, A. Passaseo, M. Lomascolo, R. Cingolani, and M. De Vittorio, Appl. Phys. Lett. **85**, 6083 (2004).
[30]M. Özdoğan, S. Yiğen, C. Çelebi, and G. Utlu, Thin Solid Films **680**, 48 (2019).
[31]M. De Vittorio, B. Potì, M. Todaro, M. Frassanito, A. Pomarico, A. Passaseo, M. Lomascolo, and R. Cingolani, Phys. Status Solidi C **1**, 589 (2004).
[32]A. Bonfiglio, G. Traetta, M. Lomascolo, A. Passaseo, and R. Cingolani, J. Appl. Phys. **89**, 5782 (2001).